ACS OMEGA

http://pubs.acs.org/journal/acsodf

Article

Quantitative Measurement Reveals Dynamic Volatile Changes and Potential Biochemical Mechanisms during Green Tea Spreading Treatment

Mingjie Chen,* Dongsheng Fang, Huan Gou, Shiya Wang, and Wenjie Yue

Cite This: *ACS Omega* 2022, 7, 40009−40020

Read Online

ACCESS | Metrics & More | Article Recommendations | Supporting Information

ABSTRACT: Quantitative data provide clues for biochemical reactions or regulations. The absolute quantification of volatile compounds in tea is complicated by their low abundance, volatility, thermal liability, matrix complexity, and instrumental sensitivity. Here, by integrating solvent-assisted flavor evaporation extraction with a gas chromatography-triple quadrupole mass spectrometry platform, we successfully established a method based on multiple reaction monitoring (MRM). The method was validated by multiple parameters, including the linear range, limit of detection, limit of quantification, precision, repeatability, stability, and accuracy. This method was then applied to measure temporal changes of endogenous volatiles during green tea spreading treatment. In total, 38 endogenous volatiles were quantitatively measured, which are derived from the shikimic acid pathway, mevalonate pathway, 2-C-methylerythritol-4-phosphate pathway, and fatty acid derivative pathway. Hierarchical clustering and heat-map analysis demonstrated four different changing patterns during green tea spreading treatment. Pathway analysis was then conducted to explore the potential biochemistry underpinning these dynamic change patterns. Our data demonstrated that the established MRM method showed high selectivity and sensitivity for quantitative tea volatile measurement and offered novel insights about volatile formation during green tea spreading.

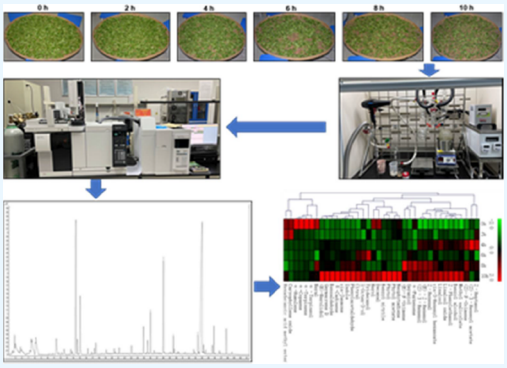

1. INTRODUCTION

Tea, which is produced from the tender shoots of *Camellia sinensis*, becomes the most popular beverage in the world after water.[1] The aroma of the tea liquor is a crucial factor that define the quality of tea.[2] The aroma compounds present in made tea are either derived from fresh tea leaves or generated by postharvest tea processing technologies.[3−5] During processing, tea leaves go through several steps, including withering, rolling, fermentation, postfermentation, and roasting (drying) to produce different types of tea.[6] For withering treatment, freshly harvested tea shoots are evenly spread on a bamboo sieve and placed in an ambient temperature or controlled environment for a certain period.[6] The purpose of withering treatment is twofold: reduce the moisture content of the leaf and induce diverse chemical changes to shape the aroma and taste characteristics of the final tea products.[7] Recently, volatile changes during the withering process have been characterized in oolong tea,[8−12] black tea,[13,14] and white tea.[15,16] These investigations established that volatile changes are very dynamic during the tea withering process. The majority of these studies were based on a head space-solid phase microextraction-gas chromatography-mass spectrometry platform (HS-SPME−GC−MS), and the volatile contents were quantified in relative proportions. Transcriptomic and metabolomics were also applied to investigate the molecular mechanisms underpinning metabolite degradation and transformation during tea withering.[17−21]

During the green tea making processes, spreading, an equivalent step to the withering of black tea, oolong tea, and white tea processing, is regularly applied. Few studies have been performed to characterize volatile changes during the spreading of green tea making. Only recently, volatile changes at five stages of green tea making were quantitatively measured by using isotopically labeled internal standards. The authors found that the spreading increased the concentrations of the alcohols as well as all aldehydes.[22] However, the volatile changes during tea spreading were not temporally resolved in that study,[22] which limits the mechanistic interpretation. The length of withering time has significant effects on metabolite degradation and transformation.[13,23,24]

For green tea making, spreading is regarded as "mild-withering"[19] and is essential to develop the mellow umami taste and delicate fragrance of green tea.[25] To date, about 270

Received: July 22, 2022
Accepted: October 11, 2022
Published: October 24, 2022

volatile compounds have been identified in green tea.[26] Due to their large differences in odor detection threshold, the contributions to the aroma quality of green tea for many of them remains unclear. Xinyang Maojian tea is a top-grade green tea produced in Xinyang, Henan province, China. The region locates to the transit zone from subtropical to continental; in addition, the region's Dabie mountain creates diverse ideal microclimates for tea growth. Xinyang Maojian tea is produced by a traditional, small-scale manufacturing process, which starts with hand-plucking of the youngest tea shoots, followed by spreading (or withering), fixing (de-enzyming), rolling, and drying. Spreading is deemed to be essential in shaping the overall characteristics of green tea. By now, the aroma formation mechanisms remain elusive, largely due to the short of the quantitative dataset regarding their changes.

Absolute quantification of volatile contents in tea can be helpful to calculate its odor activity value and clarify their contributions to the aroma quality;[27] in addition, quantitative data provide clues regarding their biochemical reactions and regulations. However, the absolute quantification of volatile compounds in tea is complicated by their low abundance, volatility, thermal liability, matrix complexity, and instrumental sensitivity. Stable isotope dilution analysis (SIDA) is the ideal choice for absolute quantification of volatiles; especially for the trace compounds such as plant volatiles, the SIDA can offer higher accuracy.[22] However, many isotope-labeled standards are inaccessible which limits its wide application. Previously, we optimized a volatile extraction procedure and then combined with the analytical power of quadrupole mass spectrometry and flame ionization detector (FID) for qualitative and quantitative analysis. In conjunction with FID response factor correction, we established a high-throughput quantitative method for tea volatile measurement.[3] Compared with a single quadrupole mass analyzer, a triple quadrupole mass analyzer can be operated in multiple reaction monitoring (MRM) mode, which has the advantage of lower noise and higher selectivity and sensitivity. Thus, the MRM method has the potential to reliably detect and quantify low abundant compounds such as tea volatiles. In this study, we developed and validated a MRM method and then applied it to measure the dynamic volatile changes during the spreading of green tea. We demonstrated that the established MRM method was robust and offered deeper insights about the biochemical transformation of tea volatiles during postharvest spreading.

2. EXPERIMENTAL SECTION

2.1. Chemicals and Materials. Anhydrous sodium sulfate (AR grade) was purchased from GHTECH (Shantou, Guangdong, China); dichloromethane (AR grade) was ordered from PN-CHEM (Zhengzhou, Henan, China). Tridecanol, 2-hexenal, 2-heptanol, (Z)-3-hexenyl acetate, decanal, and benzyl nitrile were purchased from Sigma (St. Louis, Missouri, USA); α-farnesene, cis-3-hexenyl hexanoate, 1-hexanol, (Z)-3-hexenol, benzaldehyde, phytol acetate, ethyl decanoate, 3-octanol, and guaiacol were obtained from Macklin (Shanghai, China); β-ocimene, α-copaene, germacrene D, and neophytadiene were purchased from J&K Chemicals (Shanghai, China); cis-jasmone, caffeine, and (E)-2-hexenol were obtained from ChemFaces (Wuhan, China); indole was purchased from Solarbio (Beijing, China); benzyl alcohol, linalool, geraniol, nerol, nerolidol, α-terpinene, α-humulene, hexadecanoic acid methyl ester, phytol, phenylacetaldehyde, α-terpineol, 2-phenylethanol, 1-octen-3-ol, δ-cadinene, caryophyllene oxide, neral, methyl salicylate, and linalool oxide were purchased from Yuanye Bio-Technology Co. (Shanghai, China). The alkane standard (C_6−C_{44}) was purchased from AccuStandard (New Haven, CT, USA).

2.2. Standard Solution Preparation. Nearly all volatile compounds were dissolved in anhydrous ethanol to make stock solution at 20 mg mL^{-1}; nerol, nerolidol, α-terpinene, and α-humulene were the only exceptions and prepared at 100 mg mL^{-1} in dichloromethane. The mixtures (100 μg mL^{-1} each) were prepared from stock solution and were successively diluted by half to prepare concentration gradients at 50, 25, 12.5, 6.25, 3.13, 1.56, 0.78, 0.39, 0.20, and 0.10 μg mL^{-1}. α-Terpinene, α-farnesene, linalool oxide, and nerol were the only exceptions with higher concentration gradients.

2.3. Tea Spreading Treatment. Sprouts (one bud and two leaves) of *Camellia sinensis cv Xinyang 10* were harvested from the tea garden of Xinyang Xiangyun Tea Co., Ltd. on September 27, 2021. The samples were evenly spread onto a 60 cm diameter bamboo sieve and kept indoors under fluorescence light. The tea moisture contents were monitored during tea spreading (Figure S1). Starting from spreading, the sampling was conducted at two-hour interval (0, 2, 4, 6, 8, and 10 h). At each interval, triplicates were collected into home-made aluminum foil bags, quickly frozen in liquid nitrogen, and then stored in a −80 °C freezer for volatile extraction. A second set of triplicates was harvested to measure leaf water contents. Fresh leaf weights were measured and then dried in a 90 °C oven for 24 h; the dry leaf weight was measured again. The leaf water contents were calculated by the following formula: leaf water content (%) = (fresh leaf weight − dry leaf weight) × 100/fresh leaf weight.

2.4. Tea Volatile Extraction and Separation. Tea volatile extraction follows our previous methods with minor modifications.[3,27] Fresh tea leaves (∼3.0 g) were weighed into a mortar containing 2.0 g of anhydrous sodium sulfate and ground into powder in the presence of liquid nitrogen. The tea powder was transferred into a 50-mL glass tube, and 30 mL of dichloromethane containing 0.687 μg mL^{-1} 3-octanol was added; the tube was capped and placed in a ventilation hood for 2 h to extract tea volatiles. The supernatant was transferred into a fresh glass tube and stored in a −20°C freezer.

A solvent-assisted flavor evaporation (SAFE) method was applied to separate volatile compounds from nonvolatile substances by following the previous method with minor modifications.[3] The SAFE unit head and leg temperature were maintained using38 °C water; the distillation flask was immersed in a 38 °C water bath. The distillate was collected into a fresh glass tube and stored in a −20 °C freezer. Before GC−MS analysis, the samples were concentrated using a nitrogen blower with water bath temperature setting at 37 °C. When the volume was reduced to about 2.0 mL, the solution was transferred into a 2-mL GC vial and concentrated to ∼0.5 mL under a gentle nitrogen stream. Before analysis, 5.0 μL of ethyl decanoate (4.315 μg μL^{-1}) was added into each sample. Parallelly, 5.0 μL of ethyl decanoate (4.315 μg μL^{-1}) and 5.0 μL of 3-octanol (4.125 μg μL^{-1}) were diluted into 490 μL of dichloromethane and analyzed within the same batch as other tea samples; ethyl decanoate and 3-octanol were used to calibrate the individual sample volume and recovery rate, respectively.

2.5. GC−MS Analysis. Samples were analyzed using an Agilent 7000D GC-MS Triple Quad with an Agilent 7890B

https://doi.org/10.1021/acsomega.2c04654
ACS Omega 2022, 7, 40009−40020

Table 1. Linear Range, Linear Equation, Correlation Coefficients (r^2), Limit of Detection (LOD), and Limit of Quantitation (LOQ) of the Analytes

analytes	linear range (μg mL^{-1})	linear equation[a]	r^2	LOD[b] (μg mL^{-1})	LOQ[c] (μg mL^{-1})
2-hexenal	0.10−6.25	Y = 12,503X + 5734	0.989	0.002	0.005
(Z)-3-hexenol	0.10−6.25	Y = 13,114X + 16,210	0.907	0.05	0.09
(E)-2-hexenol	0.10−6.25	Y = 138,257X − 66,372	0.963	0.014	0.047
2-heptanol	0.10−12.5	Y = 47,443X + 21,644	0.933	0.041	0.09
benzaldehyde	0.10−6.25	Y = 3,452,335X + 1,508,821	0.998	0.0002	0.0005
1-octen-3-ol	0.09−6.25	Y = 2567X + 15,601,588,518	0.939	0.038	0.09
3-octanol	0.10−6.25	Y = 308,805X + 664,905	0.976	0.0001	0.0003
(Z)-3-hexenyl acetate	0.10−6.25	Y = 383,062X + 375,625	0.996	0.0005	0.0018
α-terpinene	1.56−100	Y = 21,974X + 53,441	0.984	0.009	0.029
benzyl alcohol	0.10−6.25	Y = 2,401,730X + 986,601	0.996	0.00008	0.00028
(E)-β-ocimene	0.029−29.61	Y = 226295.0X + 245754.6	0.989	0.00286	0.00953
phenylacetaldehyde	0.10−6.25	Y = 2,552,671X + 2,841,689	0.986	0.00006	0.0002
(Z)-β-ocimene	0.069−70.4	Y = 324273.4X + 801704.7	0.990	0.0260	0.0875
linalool oxide	0.29−75	Y = 150,771X + 350,559	0.989	0.0002	0.0006
guaiacol	0.10−6.25	Y = 2,480,648X + 2,038,914	0.988	0.00002	0.00006
linalool	0.10−6.25	Y = 36,663X + 39,917	0.988	0.016	0.055
2-phenylethanol	0.10−6.25	Y = 187,352X + 1,279,455	0.992	0.00014	0.00047
benzyl nitrile	0.10−6.25	Y = 5559X + 2973	0.996	0.01	0.04
α-terpineol	0.10−6.25	Y = 687X + 497	0.992	0.009	0.02
methyl salicylate	0.10−6.25	Y = 11.1X + 5.8	0.964	0.003	0.01
decanal	0.10−6.25	Y = 70,123X + 62,236	0.989	0.0023	0.0076
nerol	0.29−37.5	Y = 766,853X + 776,122	0.986	0.0006	0.002
neral	0.021−21.37	Y = 9829.4X + 7732.6	0.986	0.0019	0.0064
geraniol	6.25−100	Y = 139,228X − 3,715,886	0.940	0.089	0.29
citral	0.077−39.3	Y = 8421.0X + 21286.0	0.991	0.0022	0.0073
indole	0.10−6.25	Y = 40,433,961X + 4,028,377	0.989	0.0003	0.0009
cis-3-hexenyl hexanoate	0.10−6.25	Y = 646,226X + 343,102	0.983	0.0004	0.0014
α-copaene	0.10−6.25	Y = 4,998,188X + 421,489	0.996	0.00004	0.00012
ethyl decanoate	0.10−6.25	Y = 91,849X + 57,260	0.980	0.0004	0.0013
cis-jasmone	0.10−6.25	Y = 158,040X + 92,478	0.993	0.04	0.012
α-humulene	0.10−6.25	Y = 74,213X + 53,785	0.991	0.001	0.004
germacrene D	0.10−6.25	Y = 313,774X − 27,382	0.996	0.003	0.011
δ-cadinene	0.10−6.25	Y = 332,923X + 145,869	0.984	0.003	0.01
α-farnesene	0.29−37.5	Y = 48.2X + 147.0	0.983	0.1	0.29
tridecanol	0.10−6.25	Y = 284.8X + 143.8	0.992	0.002	0.006
(E)-nerolidol	3.13−50	Y = 59,778X + 309,413	0.948	0.014	0.047
caryophyllene oxide	0.10−6.25	Y = 18,530X + 29,420	0.976	0.035	0.07
neophytadiene	0.10−6.25	Y = 1343X + 1404	0.979	0.03	0.09
caffeine	0.10−6.25	Y = 2,297,280X + 1,002,175	0.996	0.0005	0.0015
hexadecanoic acid, methyl ester	0.10−6.25	Y = 29,562X + 11,401	0.993	0.003	0.008
phytol	0.10−6.25	Y = 8221X + 10,701	0.961	0.009	0.02
phytol acetate	0.10−6.25	Y = 523,400X + 251,814	0.996	0.012	0.04

[a]Y represents peak area, X represents concentration of individual compound (μg mL^{-1}). [b]Signal-to-noise ratio is 3. [c]Signal-to-noise ratio is 10.

GC system; the instrument was equipped with an Agilent G4513A injector and Agilent G4514A autosampler. One microliter of sample was injected into a capillary column (HP-5MS UI, 30 m × 0.25 mm × 0.25 μm) in a splitless mode. Helium was used as the carrier gas at a constant flow rate of 1.0 mL. min^{-1}. The temperatures for the inlet, interface, and ion source were set at 240, 270, and 270 °C, respectively. The temperatures for MS Quad 1 and MS Quad 2 were set at 150 °C; the electron energy for EI-Xtr350 was set at 70 eV, and the full scan was recorded at 35−650 m/z. The oven temperature was initiated at 50 °C, held for 3 min, ramped at 5 °C min^{-1} to 180 °C, held for 2 min, ramped at 10 °C min^{-1} to 240 °C, held for 2 min, and then ramped down at 80 °C min^{-1} to 50 °C. The instrument operation and data acquisition were controlled by Mass Hunter software.

2.6. MRM Method Development for Tea Volatile Quantification. The standard volatile chemical mixture at 6.25 μg mL^{-1} was first analyzed in MS1 scan mode, and the data were analyzed by Qualitative Navigator software to get the retention time (RT) including the starting and ending time for the individual chemical standard. An appropriate precursor ion for each standard was selected based on its mass spectra. Based on RT data, the running time was divided into 32 segments. For each time segment, volatile chemicals and its precursor ion information were documented into Scan Segments. The standard volatile chemical mixture was analyzed by this new method, and the new dataset was analyzed by Qualitative Navigator software to get each precursor ion's product ion. The method was edited by selecting the scan type as MRM, and the precursor ion and corresponding product ion

https://doi.org/10.1021/acsomega.2c04654
ACS Omega 2022, 7, 40009−40020

Table 2. Precision, Repeatability, and Stability of Analytes

analytes	precision[a] (RSD, %, n = 6)				repeatability[b] (RSD, %, n = 6)	stability[c] (RSD, %, n = 6)
	intraday 1	intraday 2	intraday 3	interday		
2-hexenal	10.97	10.11	7.62	9.32	11.95	12.72
(Z)-3-hexenol	10.11	11.02	6.89	11.23	14.49	13.12
(E)-2-hexenol	9.59	3.57	3.44	5.89	10.89	13.62
1-hexanol	7.59	7.66	6.51	6.36	8.49	8.90
2-heptanol	5.75	6.56	6.57	5.96	8.29	8.33
benzaldehyde	3.04	3.14	2.73	2.94	7.68	6.60
1-octen-3-ol	4.57	5.72	1.81	4.16	17.78	14.65
3-octanol	2.59	2.26	1.95	2.46	7.79	5.74
(Z)-3-hexenyl acetate	2.13	2.00	1.76	1.96	4.13	4.44
α-terpinene	11.19	10.03	11.4	11.94	13.72	13.60
benzyl alcohol	2.63	2.50	2.2	2.92	7.02	6.81
(E)-β-ocimene	2.11	2.32	2.04	2.53	7.26	8.69
phenylacetaldehyde	1.99	2.03	2.20	2.10	5.43	5.53
(Z)-β-ocimene	3.26	3.41	3.39	3.46	8.21	8.87
linalool oxide	2.08	2.31	2.17	2.23	6.95	6.78
guaiacol	1.95	2.13	2.02	2.38	6.74	4.84
linalool	1.89	2.06	1.33	1.93	5.64	3.72
2-phenylethanol	1.80	1.92	1.66	2.41	6.01	4.01
benzyl nitrile	2.21	1.97	1.67	2.38	7.46	9.11
α-terpineol	4.43	3.03	2.27	3.22	11.71	2.64
methyl salicylate	10.69	7.33	12.82	11.8	8.79	9.61
decanal	1.37	1.52	1.50	1.47	4.31	5.88
nerol	1.54	0.81	0.94	1.17	8.73	8.19
neral	8.93	7.11	8.77	7.81	11.96	11.42
geraniol	4.45	3.71	8.56	10.45	7.97	11.67
citral	5.83	6.21	5.42	6.95	10.25	11.47
indole	1.60	1.54	1.43	1.70	5.24	9.72
cis-3-hexenyl hexanoate	1.32	1.18	1.07	1.14	8.71	2.42
α-copaene	1.79	1.74	1.69	1.92	9.71	5.11
ethyl decanoate	1.46	1.76	1.67	1.70	2.11	2.36
cis-jasmone	1.61	2.25	2.14	2.07	10.51	13.24
α-humulene	2.20	3.30	2.40	2.97	8.40	12.08
germacrene D	2.16	2.36	2.32	2.37	9.11	8.70
δ-cadinene	1.96	2.65	2.44	2.47	10.93	5.09
α-farnesene	3.17	3.89	4.66	4.02	15.92	12.93
tridecanol	11.04	5.09	8.77	10.8	16.92	14.93
(E)-nerolidol	1.63	1.93	1.77	1.81	12.91	4.35
caryophyllene oxide	5.87	1.81	3.39	4.36	4.55	12.97
neophytadiene	2.42	1.71	1.91	2.34	13.22	11.51
caffeine	1.54	1.82	2.44	2.04	6.24	11.10
hexadecanoic acid, methyl ester	2.34	2.78	2.89	2.91	13.27	4.03
phytol	7.04	4.41	6.94	6.29	15.54	13.05
phytol acetate	3.91	4.49	4.51	4.21	19.06	17.58

[a]The precision was measured by using standard mixture (6.25 μg mL^{-1}). [b,c]The repeatability and stability were measured by using volatiles extracted from fresh tea leaves.

information was documented into respective Scan Segments. The collision energy was optimized by Agilent MassHunter Design MRM Experiments Assistant software and MRM Opt-Analyze Experiments Assistant software through repeated analysis of the same standard mix with different collision energies (5, 10, 15, 20, 25, and 30 eV). The best collision energy for each ion pair was determined and applied to establish the final MRM method (Table S1).

2.7. MRM Method Validation. The MRM method was validated for linearity, limits of detection (LOD), limits of quantification (LOQ), intraday and interday precision, repeatability, stability, and accuracy.

2.7.1. Calibration Curve, LOD, and LOQ. The standard mixture gradients were analyzed in a sequence from low to high by using the above established MRM method, and the data were processed by Quant-My-Way software to make a calibration curve. For LOD and LOQ determination, the standard mixture data from the lowest concentration were analyzed by Qualitative Navigator software (B.08.00), and the signal-to-noise ratio (S/N) for the individual standard was obtained. If the S/N was above 100:1, then that standard mixture was diluted and reanalyzed until its S/N was below 100:1. The LOD and LOQ were set at S/N of 3 and 10, respectively.

https://doi.org/10.1021/acsomega.2c04654
ACS Omega 2022, 7, 40009−40020

Table 3. Recoveries of the Analytes[a]

analytes	recovery (%)			RSD (%)		
	0.1 μg g^{-1} FW	0.4 μg g^{-1} FW	4.0 μg g^{-1} FW	0.1 μg g^{-1} FW	0.4 μg g^{-1} FW	4.0 μg g^{-1} FW
benzyl alcohol	83.1	87.0	94.1	6.3	2.3	2.6
phytol	49.2	60.2	62.1	6.8	5.4	3.0
phenylacetaldehyde	60.8	57.5	50.3	8.3	8.6	2.4
α-terpineol	43.8	41.3	89.9	9.7	5.0	4.6
2-phenylethanol	56.2	58.5	68.0	4.9	1.4	2.1
1-octen-3-ol	54.1	56.8	100.2	6.6	7.9	2.1
δ-cadinene	81.3	57.9	79.6	2.6	3.6	2.9
caryophyllene oxide	63.2	47.5	56.8	10.4	8.0	9.5
neral	52.9	74.8	106.5	3.8	3.2	9.5
methyl salicylate	40.3	52.1	37.0	9.3	12.6	3.1
linalool oxide	45.6	54.9	104.2	8.4	9.0	3.3
linalool	98.0	91.9	107.1	7.2	9.1	2.9
indole	99.5	85.5	71.2	2.9	3.4	2.8
tridecanol	30.5	41.3	50.2	8.3	11.0	5.7
2-hexenal	66.7	78.2	92.5	9.1	9.4	5.6
2-heptanol	58.1	74.3	102.0	3.5	2.2	5.1
(Z)-3-hexenyl acetate	47.3	39.8	109.1	9.7	10.3	3.7
decanal	36.5	45.5	85.0	6.1	4.5	1.7
(Z)-β-ocimene	81.20	60.3	98.2	9.7	3.1	2.4
α-copaene	52.0	68.5	107.0	6.6	3.4	2.4
germacrene D	78.1	64.7	86.2	10.2	3.5	2.6
neophytadiene	63.5	71.8	70.5	1.3	2.9	3.4
cis-jasmone	84.5	69.4	79.3	8.9	6.0	3.6
caffeine	87.5	89.2	90.6	3.1	2.8	2.4
(E)-2-hexenol	61.4	65.6	58.6	5.1	5.3	4.6
α-farnesene	37.5	77.6	87.2	17.1	3.7	1.9
cis-3-hexenyl hexanoate	57.4	66.7	95.1	11.2	3.5	1.9
1-hexanol	66.1	65.0	81.8	8.2	7.8	3.7
(Z)-3-hexenol	34.5	52.9	102.6	6.3	5.7	0.6
benzaldehyde	47.8	52.9	107.6	3.4	5.7	3.7
phytol acetate	52.0	56.3	100.5	5.0	3.3	3.9
benzyl nitrile	67.6	57.2	86.0	13.9	10.8	7.1
geraniol	30.5	34.7	43.4	19.6	20.5	17.2
ethyl decanoate	70.8	75.5	73.9	5.3	1.1	3.9
3-octanol	94.3	104.1	98.9	2.1	5.5	9.3
guaiacol	82.2	94.7	95.4	6.4	5.6	4.0
(E)-β-ocimene	84.9	85.3	95.7	7.9	4.8	2.2
citral	43.8	59.2	100.1	7.3	3.61	2.8
nerol	37.3	30.1	35.4	10.8	9.5	10.4
(E)-nerolidol	31.1	40.0	70.6	19.8	14.3	3.0
α-terpinene	48.7	65.8	104.9	8.5	4.6	2.5
α-humulene	36.5	30.9	42.7	13.1	7.1	3.7
hexadecanoic acid, methyl ester	82.5	87.1	104.8	6.3	4.9	4.6

[a]FW: fresh weight.

2.7.2. Precision, Repeatability, and Stability. To determine the intraday precision, the standard mixture (6.25 μg mL^{-1}) was analyzed six times within 1 day; to determine the interday precision, the same standard mixture was analyzed six times per day and for 3 days in total. To determine the repeatability and stability, fresh tea leaves (one bud with two leaves) were harvested from the tea garden located in the Xinyang Normal University campus, and tea volatiles were extracted with the above method. To confirm the method's repeatability, one tea sample was analyzed six times. To test the method's stability, another tea sample was stored at room temperature (25 °C) and analyzed at 0, 4, 8, 12, and 24 h.

2.7.3. Accuracy. For the accuracy test, a total of 12 volatile samples were prepared from the same batch of fresh tea leaves according to the above preparation method. The fresh tea leaves were first ground into powder, and 3.0 g of tea powder was weighed into each tube. These 12 samples were divided into 4 groups (control, low spike level, medium spike level, and high spike level), and each group had triplicates. The control samples were not spiked with any standard mixture. The standard amounts equivalent to 0.1, 0.4, and 4.0 μg g^{-1} fresh weight (FW) were spiked into the tea sample before sample extraction, which represent low-, medium-, and high-spike levels, respectively. The samples were extracted and analyzed according to the above analytical method. The average recovery rates were calculated by the formula: recovery (%) = (observed amounts of spiked samples − control) × 100/spiked standard amount.

https://doi.org/10.1021/acsomega.2c04654
ACS Omega 2022, 7, 40009−40020

2.8. Hierarchical Clustering Analysis (HCA) and Heat-Map Analysis. HCA was performed by Multi Experiment Viewer software (version 4.9.0) to find relatively homogeneous clusters of metabolites based on average contents, and the content changes of metabolites were illustrated in the sequence of spreading time.

3. RESULTS AND DISCUSSION

3.1. MRM Method Validation. A typical TIC chromatogram of the volatile standards is presented in Figure S2. The linearity, LOD, LOQ, precision, repeatability, stability, and accuracy were evaluated.

3.1.1. Linearity, LOD, and LOQ. Most volatile compounds showed good linear regression from 0.1 to 6.2 μg mL^{-1} (r^2 > 0.96), while other volatiles including α-terpinene, linalool oxide, nerol, geraniol, α-farnesene, and nerolidol showed good linearity at concentrations above 0.29 μg mL^{-1}. In contrast, (E)-β-ocimene and neral showed good linear regression at concentrations down to 0.029 μg mL^{-1}. Guaiacol, which is not an endogenous tea volatile and used as an internal standard, showed the lowest LOD down to 0.00002 μg mL^{-1}; in contrast, α-farnesene, an endogenous tea volatile, showed the highest LOD up to 0.1 μg mL^{-1}. The LOQs were ranged from 0.00006 to 0.29 μg mL^{-1} (Table 1). Overall, the method was sensitive enough for quantitative analysis for all the selected volatiles.

3.1.2. Precision, Repeatability, and Stability. The precision was evaluated by repeated injection of standard mixtures (6.25 μg mL^{-1}). The relative standard deviations (RSDs) for all the selected volatiles were below 12% for the intraday and interday precision, and the majority of them were below 6% (Table 2). To test the repeatability and stability, a sample extracted from fresh tea leaves was analyzed. A representative TIC chromatogram of tea volatiles is presented in Figure S3. The RSDs for the majority of volatiles from tea samples were below 10%. Five volatiles, including 1-octen-3-ol, α-farnesene, tridecanol, phytol, and phytol acetate, showed RSDs above 15% (Table 2). Accordingly, their contents in that tea sample were quite low. Generally, the RSDs from the repeatability and stability test were higher than that of the precision test, likely due to their relative lower concentrations present in the tea samples compared with the standard mixture (6.25 μg mL^{-1} each). The data were in accordance with our previous finding that there is a negative correlation between RSDs and metabolite levels.[28]

3.1.3. Accuracy. To evaluate the accuracy of this method, volatile standard mixtures were spiked into tea samples at three different levels before sample extraction. The samples were then extracted and analyzed, and the recoveries and RSDs were calculated. The recoveries were ranged from 30.1 to 109.1%. The spike level showed diverse effects on recovery. Generally, the recovery tended to increase with the increased spike levels; however, the opposite tendency was observed for phenylacetaldehyde and indole whose recoveries were decreased with the increased spike levels. In addition, the recoveries for some volatiles were constant regardless of the spike levels; these volatiles include caryophyllene oxide, linalool, germacrene D, neophytadiene, caffeine, (E)-2-hexenol, ethyl decanoate, 3-octanol, and nerol (Table 3). The majority of RSDs from these three spike levels were below 10%, except geraniol and (E)-nerolidol whose RSDs were above 14%; both volatiles also showed lower recovery rates (Table 3). Our data indicated that the tea matrix effects on recovery are volatile-specific and concentration-dependent. Two steps during volatile extraction may have significant impacts on volatile recovery: volatile's extraction efficiency by solvent dichloromethane and the differential loss during the concentration phase of the extract. Since these selected volatiles possess different physicochemical properties (ca. solubility and volatility), this could lead to their variability in recovery (Table 3).

3.2. Volatile Changes during the Spreading of Green Tea. The tender leaves were spread for 10 h; the initial leaf water content (0 h) was 71.1%, decreased almost linearly with the progress of spreading, and reached 55.7% at 10 h spreading (Figure S1). To observe the volatile changes during the spreading of green tea, tea samples were harvested at 2 h intervals. Total volatiles were extracted and analyzed by the MRM method, and the results are presented in Table S2. To visualize the volatile changing trends, HCA and heat-map analysis were performed, and the results are presented in Figure 1. Based on their change patterns, these volatiles can be

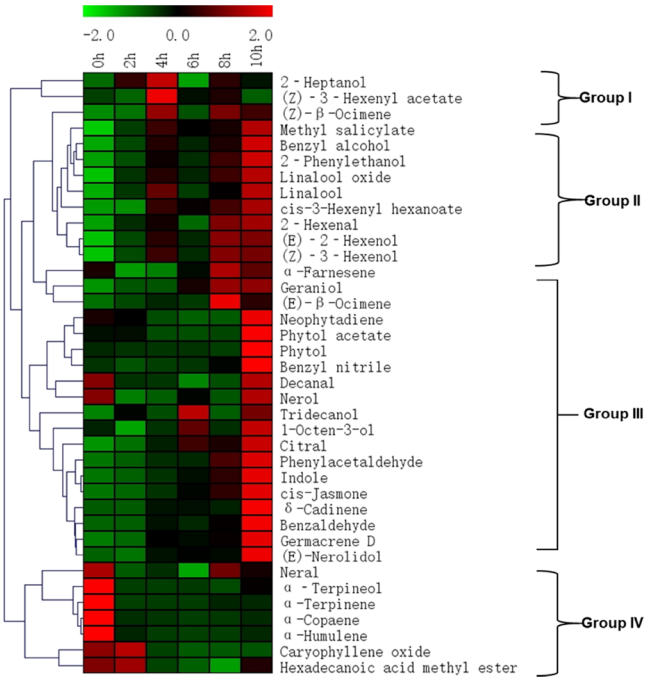

Figure 1. Hierarchical clustering analysis (HCA) and heat-map analysis of volatile changes during the spreading of green tea.

divided into four groups. The group I volatiles increased first, peaked at 4 h, and then decreased afterward. This group included 2-heptanol, (Z)-3-hexenyl acetate, and (Z)-β-ocimene. (Z)-β-Ocimene showed a second peak at 8 h spreading (Figure 1). The group II included methyl salicylate, benzyl alcohol, 2-phenylethanol, linalool oxide, linalool, cis-3-hexenyl hexanoate, 2-hexenal, (E)-2-hexenol, and (Z)-3-hexenol. These volatiles showed biphasic peaks, with the first peak at 4 h and the second peak at 8−10 h of spreading (Figure 1). The group III volatile showed a general increasing trend with the progress of spreading and peaked at 8−10 h of spreading. These volatiles include α-farnesene, geraniol, (E)-β-ocimene, neophytadiene, phytol acetate, phytol, benzyl nitrile, decanal, nerol, tridecanol, 1-octen-3-ol, citral, phenylacetaldehyde, indole, cis-jasmone, δ-cadinene, benzaldehyde, germacrene D, and (E)-nerolidol (Figure 1). The group IV volatiles showed higher contents from the fresh leaves and decreased with the progress of spreading. These volatiles included neral,

https://doi.org/10.1021/acsomega.2c04654
ACS Omega 2022, 7, 40009−40020

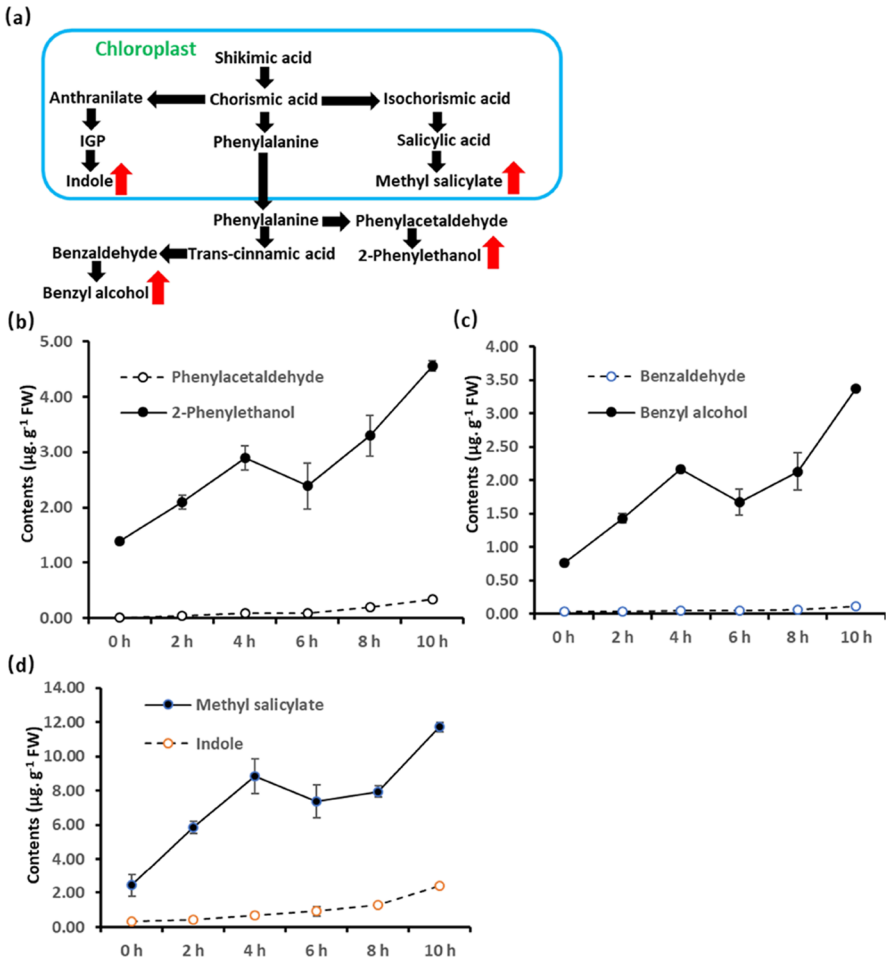

Figure 2. Dynamic changes for volatiles derived from the shikimate pathway. (a) Diagram presentation of the shikimate pathway. (b) Phenylacetaldehyde and 2-phenylethanol contents change during tea leaf spreading. (c) Benzaldehyde and benzyl alcohol contents change during tea leaf spreading. (d) Methyl salicylate and indole contents change during tea leaf spreading.

α-terpineol,α-terpinene, α-copaene, α-humulene, caryophyllene oxide, and hexadecenoic acid methyl ester (Figure 1).

3.3. Pathway Analysis Reveals Potential Mechanisms for Volatile Formation during Spreading of Green Tea. Based on their origins, these volatiles were divided into four groups, including volatiles derived from the shikimate-phenylpropanoid pathway, mevalonate (MVA) pathway, 2-C-methylerythritol-4-phosphate (MEP) pathway, and fatty acid derivative pathway.

3.3.1. Volatiles Derived from the Shikimate-Phenylpropanoid Pathway. As we observed above, group II volatiles showed biphasic changing patterns. Most group II volatiles are alcohols which can be conjugated with sugars and stored in fresh tea leaves as glycosides.[29,30] Thus, these volatile alcohols can be generated either by glycosidase-mediated cleavage or by the de novo synthesis pathway during tea spreading. The de novo synthesis is expected to result in the general increase of the intermediates and end products of that pathway. To identify the contributing pathway(s) to these volatiles' generation, volatiles derived from the same biochemical pathway were analyzed. For example, NAD-dependent alcohol dehydrogenases catalyze benzaldehyde and phenylacetaldehyde into benzyl alcohol and 2-phenylethanol, respectively (Figure 2a). From 0 to 4 h spreading, benzyl alcohol and 2-phenylethanol increased 1.4 and 1.5 $\mu g\ g^{-1}$ FW, respectively, while their aldehydes only increased 0.02 and 0.07 $\mu g\ g^{-1}$ FW, respectively (Figure 2b,c). These observations suggest that the first peak of benzyl alcohol and 2-phenylethanol at 4 h spreading mainly was generated by the glycosidase-mediated cleavage pathway, while their de novo synthesis through the shikimate pathway may also be involved. In contrast, at 10 h spreading, the contents of benzaldehyde and phenylacetaldehyde were doubled compared to that of 4 h; the contents of benzyl alcohol and 2-phenylethanol increased 56 and 57%, respectively. These data suggest that the second peaks of 2-phenylethanol and benzyl alcohol at 10 h spreading likely were mainly produced by the de novo synthesis pathway. At 6 h spreading, the contents of 2-phenylethanol and benzyl alcohol were decreased, while their aldehydes remained constant (Figure 2b,c). This drop may result from their emission into the atmosphere. Generally, the contents of 2-phenylethanol and benzyl alcohol were more than ten-fold higher compared to their respective aldehydes, suggesting that the NAD-dependent alcohol dehydrogenases catalyze the reaction toward alcohol formation. Thus, this enzyme's characteristics affect their respective alcohol-to-aldehyde ratio.

Methyl salicylate is synthesized by the methylation of salicylate (SA) and catalyzed by salicylic acid carboxyl methyltransferase.[16] SA can be converted into SA glucoside through SA glucosyltransferase activity,[31] while SA glucoside also can be hydrolyzed by SA 3-hydroxylase to release SA.[32] Methyl SA was biphasic with the first peak present at 4 h

https://doi.org/10.1021/acsomega.2c04654
ACS Omega 2022, 7, 40009−40020

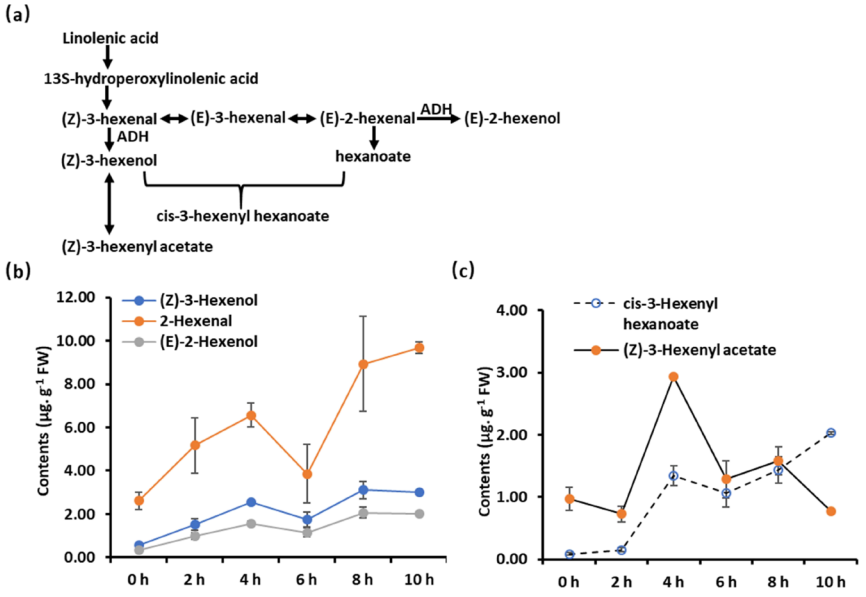

Figure 3. Dynamic changes for volatiles derived from fatty acid degradation. (a) Diagram presentation of the green leaf volatile synthesis pathway. (b) (Z)-3-Hexenol, 2-hexenal, and (E)-2-hexenol content changes during spreading. (c) cis-3-Hexenyl hexanoate and (Z)-3-hexenyl acetate content changes during spreading.

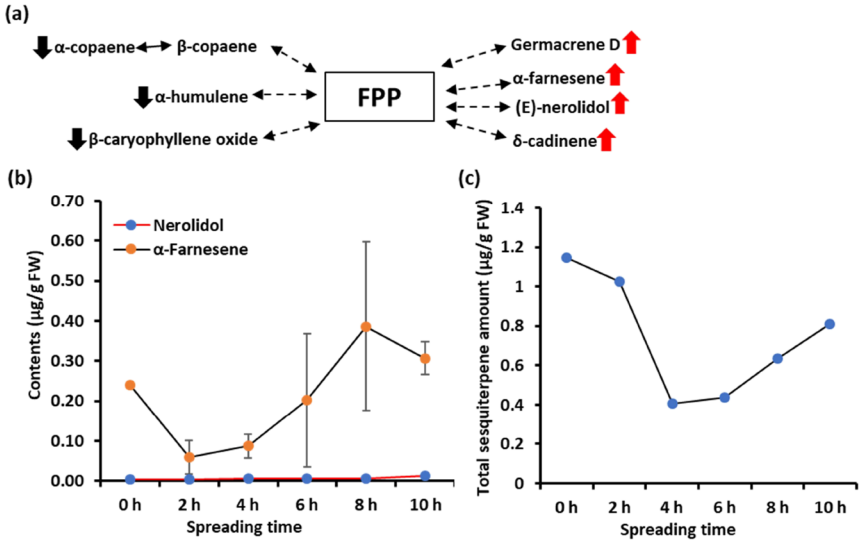

Figure 4. Dynamic changes for volatiles derived from the MVA pathway. (a) Diagram presentation of sesquiterpene synthesis. (b) (E)-Nerolidol and α-farnesene content changes during spreading. (c) Total sesquiterpene content changes during spreading.

spreading. The first methyl SA peak could be formed through SA release from SA glycoside followed by methylation, and the second peak could result from the enhanced de novo SA synthesis (Figure 2d). Similar to methyl SA, indole also is derived from chorismic acid through a branched pathway (Figure 2a). Unlike methyl SA, the indole content kept increasing during 10 h of spreading (Figure 2d). Since no indole glycoside has been reported from fresh tea leaves, this may explain why indole did not show a peak at 4 h spreading.

Phenylalanine is the precursor of benzyl alcohol and 2-phenylethanol synthesis (Figure 2a). Its content was highly increased during tea withering through up-regulation of chorismite mutase, prephenate dehydratase, and tryptophan synthase.[14,23] This would provide abundant intermediates for indole, methyl SA, and phenylpropanoid synthesis at the late stage of tea withering. These data suggest that shikimic acid-derived aroma synthesis during green tea spreading could be regulated at the transcriptional level and by substrate availability.

3.3.2. Volatiles Derived from the Fatty Acid Derivative Pathway. Four volatiles from the fatty acid derivative pathway (Figure 3a), including 2-hexenal, (E)-2-hexenol, (Z)-3-hexenol, and cis-3-hexenyl hexanoate, showed biphasic changes in group II volatiles (Figure 1). ADH catalyzes 2-hexenal to (E)-2-hexenol (Figure 3a);[8] both showed highly correlated trends during 10 h of spreading (Figure 3b), suggesting that fatty acid degradation was initiated at the beginning of spreading, and account for the increase of these green leaf volatiles (GLVs). The 2-hexenal contents were more than threefold higher than that of (E)-2-hexenol at any time point, suggesting that ADH catalyzes a reversible reaction toward aldehyde formation. Thus, ADH enzyme characteristics affect

https://doi.org/10.1021/acsomega.2c04654
ACS Omega 2022, 7, 40009−40020

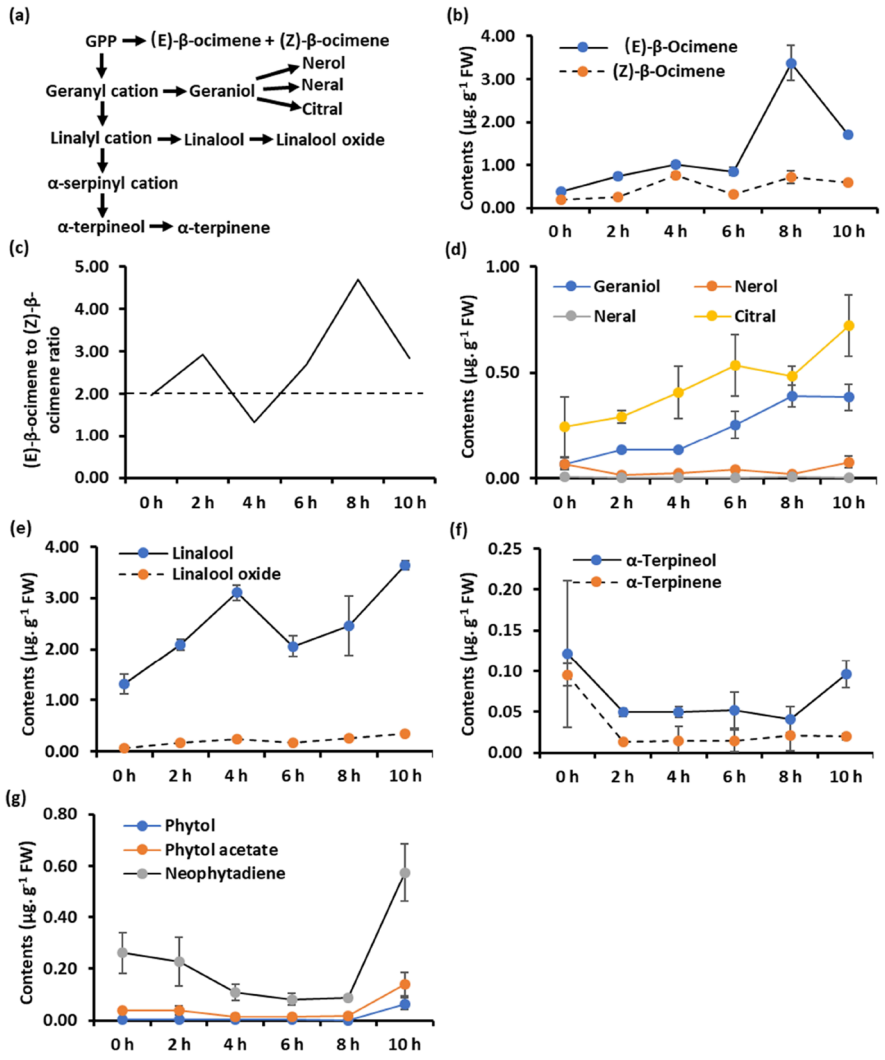

Figure 5. Dynamic changes for volatiles derived from the MEP pathway. (a) Diagram presentation of monoterpene synthesis from GPP. (b) (E)-*β*-Ocimene and (Z)-*β*-ocimene content changes during spreading. (c) The (E)-*β*-ocimene-to-(Z)-*β*-ocimene ratio changes during spreading. (d) Geraniol, nerol, neral, and citral content changes during spreading. (e) Linalool and linalool oxide content changes during spreading. (f) *α*-Terpineol and *α*-terpinene content changes during spreading. (g) Phytol, phytol acetate, and neophytadiene content changes during spreading.

the aldehyde-to-alcohol ratio of these GLVs. (Z)-3-Hexenol glycoside has been isolated from tea (cv. *Yabukita*),[33] although its presence *Xinyang 10* cultivar remains unclear. 2-Hexenal, (E)-2-hexenol, and (Z)-3-hexenol showed highly correlated changing patterns (Figure 3b), suggesting that the major source for these GLVs was through de novo fatty acid degradation, while glycosidase(s)-mediated cleavage of their glycoside precursors may play a minor role during green tea spreading.

cis-3-Hexenyl hexanoate contents increased 25-fold during 10 h spreading; (Z)-3-hexenyl acetate content increased threefold during the first 4 h spreading (Figure 3c), suggesting that considerable amounts of newly formed (Z)-3-hexenol were converted and stored in the ester forms. cis-3-Hexenyl hexanoate synthesis also require hexanoate as the substrate, which could be synthesized through 2-hexenal oxidization. After 4 h spreading, the (Z)-3-hexenyl acetate content decreased (Figure 3c); this reduction could result from its emission into the atmosphere or ester bond cleavage. In the latter case, (Z)-3-hexenol would show a higher peak at 6 h after its release from its ester precursor. However, (Z)-3-hexenol content was lower at 6 h compared with 4 h (Figure 3b), suggesting that (Z)-3-hexenyl acetate ester bond cleavage may not have happened.

3.3.3. Volatiles Derived from the MVA Pathway. Sesquiterpenes are derived from the MVA pathway. In this study, seven sesquiterpenes were detected and quantified; they are *α*-copaene, *α*-humulene, caryophyllene oxide, *α*-farnesene, *δ*-cadinene, germacrene D, and nerolidol (Table S2). The cytosolic FPP pool is the common intermediate for their synthesis (Figure 4a). *α*-Copaene, *α*-humulene, and caryophyllene oxide were higher in fresh tea leaves and declined within the first 2 h of spreading; in contrast, germacrene D, *α*-farnesene, (E)-nerolidol, and *δ*-cadinene contents increased as spreading continued (Figures 1 and 4a). In *Arabidopsis*, a recombinant terpene synthase (TPS) encoded by At5g23960 catalyzes FPP into (−)-*α*-copaene, *α*-humulene, and (−)-E-caryophyllene;[34] we speculate that a tea homolog of At5g23960 may exist and catalyze a similar reaction. The concerted changes of these three sesquiterpenes during tea spreading are in accordance with this speculation.

CsAFS catalyzes *α*-farnesene synthesis, and its expression was induced by wounding stress.[35] (E)-Nerolidol synthase (CsNES) catalyzes (E)-nerolidol synthesis,[36] and its tran-

https://doi.org/10.1021/acsomega.2c04654
ACS Omega 2022, 7, 40009−40020

scription was up-regulated during oolong tea processing. Here, we found that α-farnesene was present in fresh tea leaves at a relatively high level and exhibited a pattern of decreasing first then increasing; in contrast, (E)-nerolidol showed a mild increasing trend during spreading (Figure 4b). The different changing trends of nerolidol and α-farnesene during green tea spreading support their independent synthesis.[35,36] Our data also suggest that the induction of *CsAFS* could be faster and stronger compared to *CsNES* induction.

Since FPP is the common intermediate for the synthesis of all seven sesquiterpenes, the opposite temporal changing patterns raised intriguing question about de novo sesquiterpene synthesis and the reversibility of TPS-catalyzed reactions. In planta, FPP is maintained at trace levels.[37,38] If TPS catalyzes a reversible reaction, these seven sesquiterpenes could be interconverted through FPP (Figure 4a). Under this scenario, the total sesquiterpene content would remain constant; in contrast, if de novo FPP synthesis were operated during tea spreading, the total sesquiterpene content is expected to increase. We calculated the total sesquiterpene contents at each sampling point; the fresh tea leaves contained the highest level of total sesquiterpene and exhibited a decreasing trend during the first 4 h spreading followed by an increasing trend. At the end of spreading, the total sesquiterpene content still was lower than that of fresh tea leaves (Figure 4c). If TPS-mediated reactions were reversible, fresh tea leaves essentially contain sufficient amounts of total sesquiterpenes to sustain their interconversion through FPP. Under such circumstances, the de novo FPP synthesis would be not involved. However, there are two issues with this hypothesis: (1) within the first 4 h of spreading, caryophyllene oxide and α-farnesene are the major contributors to the twofold reduction of the total sesquiterpene content (Table S1). They may be emitted into the atmosphere and thus cannot be recycled for other sesquiterpene conversion. (2) From 6 to 10 h spreading, the total sesquiterpene content increased (Figure 4c). Thus, additional FPP should be generated de novo to drive the increase. Meanwhile, other factors should be taken into account which could support this hypothesis: (1) the targeted metabolic profiling in this study could miss some unidentified sesquiterpenes which are involved in the sesquiterpene interconversion; (2) sesquiterpene glycosides and esters have been found from other plant species;[39−44] they could also be present in fresh tea leaves. During 4 to 10 h spreading, these compounds could be released by glycosidases and contribute to the total sesquiterpene increase. Obviously, further work is required to clarify this issue.

3.3.4. Volatiles Derived from the MEP Pathway. Ten monoterpenes and three diterpenes were detected from fresh tea leaves of *Xinyang 10* cultivar (Table S2). They are synthesized from GPP or GGPP which are derived from the MEP pathway in plastids (Figure 5a). A tea *CsOCS* (TEA014989.1) and snapdragon (*ama0a23*) encodes (E)-β-ocimene synthase; both catalyze GPP to produce predominantly (E)-β-ocimene and a small amount of (Z)-β-ocimene.[40,45] In this study, both (E)-β-ocimene and (Z)-β-ocimene were detected, and both showed biphasic peaks at 4 and 8 h spreading (Figures 1 and 5b). From 0 to 6 h, the ratio of (E)-β-ocimene to (Z)-β-ocimene was around 2 and increased to 5 at 8 h of spreading (Figure 5c). The in vitro enzyme activity assay demonstrated that recombinant ama0a23 or CsOCS protein produces (E)-β-ocimene and (Z)-β-ocimene in a ratio of 97:2;[40,45] in contrast, recombinant CsOCS2 (TEA004606.1) produces both (E)-β-ocimene and (Z)-β-ocimene in a relative abundance about 2:1.[46] Our data suggest that before 4 h of spreading, CsOCS2 was the dominant enzyme responsible for ocimene synthesis; after 4 h of spreading, *CsOCS* could be induced and result in the (E)-β-ocimene increase. At 10 h of spreading, the ratio of (E)-β-ocimene to (Z)-β-ocimene decreased to 2.8, suggesting that CsOCS activity could be deactivated after 8 h of spreading, or after 8 h of spreading, most of the newly synthesized (E)-β-ocimene was emitted into the atmosphere.

Geraniol showed a general increasing trend during green tea spreading (Figures 1 and 5d). There are two potential pathways for geraniol formation: de novo synthesis or glycosidase-mediated precursor cleavage; it remains unresolved which one contributes to its increase in this study. Geraniol can be further converted to nerol, neral, or citral (Figure 5a). Nerol and neral were detected at trace amounts, and the citral content was higher than that of geraniol (Figure 5d), suggesting that most geraniol was converted into citral during green tea spreading.

Linalool contents showed biphasic peaks during green spreading, with the first peak present at 4 h (Figure 5e). Starting from 6 h of spreading, the linalool content increased again. Considering that linalool glycosides were found from fresh tea leaves,[30] the biphasic peaks could be resulted from enhanced de novo linalool synthesis or glycosidase-mediated cleavage. The linalool oxide is synthesized from linalool and catalyzed by linalool oxygenase; its content kept around 10% of linalool at any sampling points, suggesting that the linalool oxide is mainly regulated by substrate availability; linalool oxygenase may not be the committing step for linalool oxide synthesis.

α-Terpineol and α-terpinene were present at higher content in fresh tea leaves and declined sharply within 2 h of tea spreading; we speculate that this reduction could be caused by their emission into the atmosphere (Figure 5f). From 2 to 8 h of spreading, both contents remained constant; after 8 h spreading, the α-terpineol content increased again (Figure 5f). These data suggest that the responsible enzymes converting linalool cations or α-terpinyl cations into α-terpineol were activated only after 8 h of spreading (Figure 5a).

Three diterpenes, including phytol, phytol acetate, and neophytadiene, were measured in this study. Free phytol is toxic to plants; we found that it was present at trace amounts in fresh tea leaves and mainly stored in phytol acetate form. Neophytadiene was the major diterpene detected from fresh tea leaves (Figure 5g). Interestingly, these three diterpenes showed highly synchronized changing patterns: their contents gradually decreased until 8 h of spreading followed by a rapid increase (Figure 5g). Yu et al.[47] reported that at the initial stage of withering, the chlorophyll synthesis pathway was up-regulated by mild-dehydration stress, and the chlorophyll content was significantly increased; at the late withering stage, chlorophyll degradation was initiated. Thus, our data showed that these diterpene contents were negatively correlated with chlorophyll synthesis and positively correlated with chlorophyll degradation. During chlorophyll synthesis, free phytol can be recycled and integrated into chlorophyll; during chlorophyll degradation, phytol can be released from chlorophyll by chlorophyll dephytolase CLD1;[48] the released free phytol could be acylated into phytol acetate or converted into neophytadiene. Although the neophytadiene synthesis path-

https://doi.org/10.1021/acsomega.2c04654
ACS Omega 2022, 7, 40009−40020

ways remain unresolved, our data suggest that it likely serves as an intermediate of the phytol degradation pathway; it also could be mobilized for chlorophyll synthesis.

4. CONCLUSIONS

In this study, we established a GC-TQS-based MRM method for quantitative volatile measurement in tea by coupling with SAFE extraction. We validated this method's performances by various parameters, including the calibration curve, LOD, LOQ, precision, repeatability, stability, and accuracy. As a proof of concept, we applied this MRM method to quantify 38 endogenous volatiles during postharvest spreading of green tea making. Through hierarchical clustering and heat-map analysis, we identified four volatile changing patterns during spreading. Through pathway analysis, the potential causes for these dynamic volatile changes were discussed. Overall, our quantitative dataset was in accordance with previous reports and also raised new questions or hypothesis for future investigation. Collectively, we demonstrated that this established MRM volatile measurement method was robust and could be readily adapted for quantitative volatile measurement from other horticultural plants or the food matrix.

■ ASSOCIATED CONTENT

Supporting Information

The Supporting Information is available free of charge at https://pubs.acs.org/doi/10.1021/acsomega.2c04654.

The spreading treatment and water content changes of fresh tea leaves (Figure S1), the total ion chromatography results of the standard volatile mixture selected in this study (Figure S2), the total ion chromatography results of volatiles extracted from fresh tea leaves (Figure S3), the MRM method parameters (Table S1), and the tea volatile content changes during 10-h spreading treatment (Table S2) (PDF)

■ AUTHOR INFORMATION

Corresponding Author

Mingjie Chen − *College of Life Sciences, Henan Key Laboratory of Tea Plant Biology, Xinyang Normal University, Xinyang, Henan 464000, China;* orcid.org/0000-0002-3302-934X; Email: mjchen@xynu.edu.cn

Authors

Dongsheng Fang − *College of Life Sciences, Henan Key Laboratory of Tea Plant Biology, Xinyang Normal University, Xinyang, Henan 464000, China*

Huan Gou − *College of Life Sciences, Henan Key Laboratory of Tea Plant Biology, Xinyang Normal University, Xinyang, Henan 464000, China*

Shiya Wang − *College of Life Sciences, Henan Key Laboratory of Tea Plant Biology, Xinyang Normal University, Xinyang, Henan 464000, China*

Wenjie Yue − *Jinshan College, Fujian Agriculture and Forestry University, Fuzhou, Fujian 350002, China*

Complete contact information is available at: https://pubs.acs.org/10.1021/acsomega.2c04654

Author Contributions

M.J.C. conceived and designed the experiments; D.S.F., H.G., S.Y.W., and W.J.Y. performed experiments and analyzed the data; M.J.C. wrote the manuscript.

Notes

The authors declare no competing financial interest.

■ ACKNOWLEDGMENTS

This research was supported by Key-Area Research and Development Program of Guangdong Province (2020B020220004), Opening Funding of Guangdong Key Laboratory of Tea Plant Resources Innovation & Utilization (2020KF06), and National Science Foundation of China (31870803). The authors thank Xinyang Xiangyun Tea Co., Ltd. for providing tea samples, Prof. Hongyu Yuan, Dr. Qiying Zhou, and Wei Zhang for suggestions with tea spreading treatments, and Mr. Zijian Chen (zijian.chen@hitachi-powergrids.com) from Hitachi ABB Power Grids Co. for English language editing.

■ REFERENCES

(1) Deb, S.; Pou, K. R. J. A review of withering in the processing of black tea. *J. Biosyst. Eng.* **2016**, *41*, 365−372.

(2) Zheng, X. Q.; Li, Q. S.; Xiang, L. P.; Liang, Y. R. Recent advances in volatiles of teas. *Molecules* **2016**, *21*, 338.

(3) Chen, X. B.; Zhang, Y.; Du, Z. H.; Liu, R. M.; Guo, L.; Chen, C. S.; Wu, H. L.; Chen, M. J. Establishing a quantitative volatile measurement method in tea by integrating sample extraction method optimization and data calibration. *Flavour Fragrance J.* **2020**, *36*, 64−74.

(4) Yang, Z. Y.; Baldermann, S.; Watanabe, N. Recent studies of the volatile compounds in tea. *Food Res. Int.* **2013**, *2*, 585−599.

(5) Zeng, L. T.; Watanabe, N.; Yang, Z. Y. Understanding the biosynthesis and stress response mechanisms of aroma compounds in tea (*Camellia sinensis*) to safely and effectively improve tea aroma. *Crit. Rev. Food Sci. Nutr.* **2019**, *59*, 2321−2334.

(6) Zhang, L.; Ho, C. T.; Zhou, J.; Santos, J. S.; Armstrong, L.; Granato, D. Chemistry and biological activities of processed *Camellia sinensis* teas: A comprehensive review. *Compr. Rev. Food Sci. Food Saf.* **2019**, *18*, 1474−1495.

(7) Zhen, Y. S. Tea: bioactivity and therapeutic potential (Medicinal and aromatic plants- industrial profiles). *Econ. Bot.* **2003**, *59*, 89−89.

(8) Zhou, Z. W.; Wu, Q. Y.; Yao, Z. L.; Deng, H. L.; Liu, B. B.; Yue, C.; Deng, T. T.; Lai, Z. X.; Sun, Y. Dynamics of ADH and related genes responsible for the transformation of C6-aldehydes to C6-alcohols during the postharvest process of oolong tea. *Food Sci. Nutr.* **2020**, *8*, 104−113.

(9) Hu, C. J.; Li, D.; Ma, Y. X.; Zhang, W.; Chen, L.; Zheng, X. Q.; Liang, Y. R.; Lu, J. L. Formation mechanism of the oolong tea characteristic aroma during bruising and withering treatment. *Food Chem.* **2018**, *269*, 202−211.

(10) Ma, C. Y.; Li, J. X.; Chen, W.; Wang, W. W.; Qi, D. D.; Pang, S.; Miao, A. Q. Study of the aroma formation and transformation during the manufacturing process of oolong tea by solid-phase microextraction and gas chromatography−mass spectrometry combined with chemometrics. *Food Res. Int.* **2018**, *108*, 413.

(11) Guo, X. Y.; Hod, C. T.; Wan, X. C.; Zhu, H.; Liu, Q.; Wen, Z. Changes of volatile compounds and odor profiles in Wuyi rock tea during processing. *Food Chem.* **2021**, *341*, No. 128230.

(12) Liu, Z. B.; Chen, F. C.; Sun, J. Y.; Li, N. Dynamic changes of volatile and phenolic components during the whole manufacturing process of Wuyi Rock tea (Rougui). *Food Chem.* **2022**, *367*, No. 130624.

(13) Netzimana, B.; Li, Y.; He, C.; Yu, X.; Zhou, J.; Chen, Y.; Yu, Z.; Ni, D. Different withering times affect sensory qualities, chemical components, and nutritional characteristics of black tea. *Foods* **2021**, *10*, 2627.

(14) Wu, H. L.; Huang, W. J.; Chen, Z. J.; Chen, Z.; Shi, J. F.; Kong, Q.; Sun, S. L.; Jiang, X. H.; Chen, D.; Yan, S. J. GC−MS-based metabolomic study reveals dynamic changes of chemical compositions during black tea processing. *Food Res. Int.* **2019**, *120*, 330−338.

(15) Chen, Q. C.; Zhu, Y.; Dai, W. D.; Lv, H. P.; Mu, B.; Li, P. L.; Tan, J. F.; Ni, D. J.; Lin, Z. Aroma formation and dynamic changes during white tea processing. *Food Chem.* **2018**, *274*, 915−924.
(16) Deng, W. W.; Wang, R. X.; Yang, T. Y.; Jiang, L. N.; Zhang, Z. Z. Functional characterization of salicylic acid carboxyl methyltransferase from *Camellia sinensis*, providing the aroma compound of methyl salicylate during withering process of white tea. *J. Agric. Food Chem.* **2017**, *65*, 11036−11045.
(17) Wu, Z. J.; Ma, H. Y.; Zhuang, J. iTRAQ-based proteomics monitors the withering dynamics in postharvest leaves of tea plant (*Camellia sinensis*). *Mol. Genet. Genomics* **2018**, *293*, 45−59.
(18) Zhu, C.; Zhang, S. T.; Fu, H. F.; Zhou, C. Z.; Chen, L.; Li, X. Z.; Lin, Y. L.; Lai, Z. X.; Guo, Y. Q. Transcriptome and phytochemical analyses provide new insights into long non-coding RNAs modulating characteristic secondary metabolites of oolong tea (*Camellia sinensis*) in solar-withering. *Front. Plant Sci.* **2019**, *10*, 1638.
(19) Wang, Y.; Zheng, P. C.; Liu, P. P.; Song, X. W.; Guo, F.; Li, Y. Y.; Ni, D. J.; Jiang, C. J. Novel insight into the role of withering process in characteristic flavor formation of teas using transcriptome analysis and metabolite profiling. *Food Chem.* **2019**, *272*, 313−322.
(20) Xu, P.; Su, H.; Zhao, S. Q.; Jin, R.; Cheng, H. Y.; Xu, A. A.; Lai, W. Y.; Yin, X. R.; Wang, Y. F. Transcriptome and phytochemical analysis reveals the alteration of plant hormones, characteristic metabolites, and related gene expression in tea (*Camellia sinensis L.*) leaves during withering. *Plants* **2020**, *9*, 204.
(21) Lin, J. Z.; Liu, F.; Zhou, X. F.; Tu, Z.; Chen, L.; Wang, Y. W.; Yang, Y. F.; Wu, X.; Lv, H. W.; Zhu, H. K.; Ye, Y. Effect of red light on the composition of metabolites in tea leaves during the withering process using untargeted metabolomics. *J. Sci. Food Agric.* **2021**, *102*, 1628−1639.
(22) Flaig, M.; Schieberle, P. Characterization of the key odorants in a high-grade Chinese green tea beverage (*Camellia sinensis; Jingshan cha*) by means of the sensomics approach and elucidation of odorant changes in tea leaves caused by the tea manufacturing process. *J. Agric. Food Chem.* **2020**, *68*, 5168−5179.
(23) Ye, Y.; Dong, C.; Luo, F.; Cui, J.; Liao, X.; Lu, A.; Yan, J.; Mao, S.; Li, M.; Fang, C.; Tong, H. Effects of withering on the main physical properties of withered tea leaves and the sensory quality of congou black tea. *J. Texture Stud.* **2020**, *51*, 542−553.
(24) Chaturvedula, V. S. P.; Prakash, I. The aroma, taste, color and bioactive constituents of tea. *J. Med. Plants Res.* **2011**, *5*, 2110−2124.
(25) Han, Z. X.; Rana, M. M.; Liu, G. F.; Gao, M. J.; Li, D. X.; Wu, F. G.; Li, X. B.; Wan, X. C.; Wei, S. Green tea flavor determinants and their changes over manufacturing processes. *Food Chem.* **2016**, *212*, 739−748.
(26) Nijssen, L. M.; van Ingen-Visscher, C. A.; Donders, J. J. H. *VCF volatile compounds in food: Database version 16.4*; TNO Triskelion B.V.: Zeist, The Netherlands, 2017.
(27) Chen, M. J.; Guo, L.; Zhou, H. W.; Guo, Y. L.; Zhang, Y.; Lin, Z.; Sun, M.; Zeng, W.; Wu, H. L. Absolute quantitative volatile measurement from fresh tea leaves and the derived teas revealed contributions of postharvest synthesis of endogenous volatiles for the aroma quality of made teas. *Appl. Sci.* **2021**, *11*, 613.
(28) Chen, M. J.; Rao, R. S. P.; Zhang, Y. M.; Zhong, X. K.; Thelen, J. J. A modified data normalization method for GC-MS-based metabolomics to minimize batch variation. *Springerplus* **2014**, *3*, 439.
(29) Tikunov, Y. M.; de Vos, R. C. H.; Paramas, A. M. G.; Hall, R. D.; Bovy, A. G. A role for differential glycoconjugation in the emission of phenylpropanoid volatiles from tomato fruit discovered using a metabolic data fusion approach. *Plant Physiol.* **2010**, *152*, 55−70.
(30) Moon, J. H.; Watanabe, N.; Sakata, K.; Yagi, A.; Ina, K.; Luo, S. J. Studies on the aroma formation mechanism of oolong tea. 3. Translinalool and *cis*-linalool 3,6-oxide 6-O-β-D-xylopyranosyl-β-D-glucopyranosides isolated as aroma precursors from leaves for oolong tea. *Biosci., Biotechnol., Biochem.* **1994**, *58*, 1742−1744.
(31) Lim, E. K.; Doucet, C. J.; Li, Y.; Elias, L.; Worrall, D.; Spencer, S. P.; Ross, J.; Bowles, D. J. The activity of Arabidopsis glycosyltransferases towards salicylic acid, 4-hydroxybenzoic acid and other benzoates. *J. Biol. Chem.* **2002**, *277*, 586.
(32) Zhang, Y. J.; Zhao, L.; Zhao, J. Z.; Li, Y. J.; Wang, J. B.; Guo, R.; Gan, S. S.; Liu, C. J.; Zhang, K. W. S5H/DMR6 encodes a salicylic acid 5-hydroxylase that fine-tunes salicylic acid homeostasis. *Plant Physiol.* **2017**, *175*, 1082−1093.
(33) Kobayashi, A.; Kubota, K.; Joki, Y.; Wada, E.; Wakabayashi, M. (Z)-3-hexenyl-β-D-glucopyranoside in fresh tea leaves as a precursor of green odor. *Biosci., Biotechnol., Biochem.* **1994**, *58*, 592−593.
(34) Chen, F.; Tholl, D.; D'Auria, J. C.; Farooq, A.; Pichersky, E.; Gershenzon, J. Biosynthesis and emission of terpenoid volatiles from Arabidopsis flowers. *Plant Cell* **2003**, *15*, 481−494.
(35) Wang, X. W.; Zeng, L. T.; Liao, Y. Y.; Li, J. L.; Tang, J. C.; Yang, Y. C. Formation of α-farnesene in tea (*Camellia sinensis*) leaves induced by herbivore-derived wounding and its effect on neighboring tea plants. *Int. J. Mol. Sci.* **2019**, *20*, 4151.
(36) Zhou, Y.; Zeng, L. T.; Liu, X. Y.; Gui, J. D.; Mei, X.; Fu, X. M.; Dong, F.; Tang, J. C.; Zhang, L. Y.; Yang, Z. Y. Formation of (E)-nerolidol in tea (*Camellia sinensis*) leaves exposed to multiple stresses during tea manufacturing. *Food Chem.* **2017**, *231*, 78−86.
(37) Wu, S. Q.; Schalk, M.; Clark, A.; Miles, R. B.; Coates, R.; Chappell, J. Redirection of cytosolic or plastidic isoprenoid precursors elevates terpene production in plants. *Nat. Biotechnol.* **2006**, *24*, 1441−1447.
(38) Aharoni, A.; Giri, A. P.; Deuerlein, S.; Griepink, F.; de Kogel, W. J.; Verstappen, F. W. A.; Verhoeven, H. A.; Jongsma, M. A.; Schwab, W.; Bouwmeestera, H. J. Terpenoid metabolism in wild-type and transgenic Arabidopsis plants. *Plant Cell* **2003**, *15*, 2866−2884.
(39) Huang, L. P.; Luo, D. Z.; Fu, R. R.; Yan, B.; Wang, X. B.; Shu, J. C.; Deng, J.; Huang, H. A sesquiterpene glycoside and phenylalanine derivatives from *Tinospora sinensis*. *Fitoterapia* **2019**, *137*, 104247−104247.
(40) Chen, S.; Xie, P. F.; Li, Y. Y.; Wang, X. X.; Liu, H. H.; Wang, S. S.; Han, W. B.; Wu, R. M.; Li, X. L.; Guan, Y. F.; Yang, Z. B.; Yu, X. M. New insights into stress-induced β-ocimene biosynthesis in tea (*Camellia sinensis*) leaves during oolong tea processing. *J. Agric. Food Chem.* **2021**, *69*, 11656−11664.
(41) Qi, S. Z.; Yang, Y. R.; Xian, X. Y.; Li, X. Z.; Gao, H. Y. A new sesquiterpenoid glycoside from Saussurea involucrata. *Nat. Prod. Res.* **2020**, *34*, 943−949.
(42) Wang, J. M.; Zhang, N.; Zhao, M. Y.; Jing, T. T.; Jin, J. Y.; Wu, B.; Wan, X. C.; Schwab, W.; Song, C. K. Carotenoid Cleavage Dioxygenase 4 catalyzes the formation of carotenoid-derived volatile β-ionone during tea (*Camellia Sinensis*) withering. *J. Agric. Food Chem.* **2020**, *68*, 1684−1690.
(43) Wei, S. P.; Ji, Z. Q.; Zhang, J. W. A new insecticidal sesquiterpene ester from Celastrus angulatus. *Molecules* **2009**, *14*, 1396−1403.
(44) Borbone, N.; Borrelli, F.; Montesano, D.; Izzo, A. A.; Marino, S. D.; Capasso, R.; Zollo, F. Identification of a new sesquiterpene polyol ester from Celastrus paniculatus. *Planta Med.* **2007**, *73*, 792−794.
(45) Dudareva, N.; Martin, D.; Kish, C. M.; Kolosova, N.; Gorenstein, N.; Fäldt, J.; Miller, B.; Bohlmann, J. (E)-β-ocimene and myrcene synthase genes of floral scent biosynthesis in Snapdragon: function and expression of three terpene synthase genes of a new terpene synthase subfamily. *Plant Cell* **2003**, *15*, 1227−1241.
(46) Xu, Q. S.; He, Y. X.; Yan, X. M.; Zhao, S. Q.; Zhu, J. Y.; Wei, C. L. Unraveling a crosstalk regulatory network of temporal aroma accumulation in tea plant (*Camellia sinensis*) leaves by integration of metabolomics and transcriptomics. *Environ. Exp. Bot.* **2018**, *149*, 81−94.
(47) Yu, X. L.; Hu, S.; He, C.; Zhou, J. T.; Qu, F. F.; Ai, Z. Y.; Chen, Y. Q.; Ni, D. J. Chlorophyll metabolism in postharvest tea (*Camellia sinensis. L*) leaves: variations in color values, chlorophyll derivatives and gene expression levels under different withering treatments. *J. Agric. Food Chem.* **2019**, *67*, 10624−10636.
(48) Lin, Y. P.; Wu, M. C.; Charng, Y. Y. Identification of chlorophyll dephytylase involved in chlorophyll turnover in Arabidopsis. *Plant Cell* **2016**, *28*, 2974−2990.

https://doi.org/10.1021/acsomega.2c04654
ACS Omega 2022, 7, 40009−40020